

# Influence of technological parameters on evolution of phases in Al-CMA composites prepared by powder metallurgy

I. Černíčková<sup>1\*</sup>, L. Roščák<sup>1</sup>, F. Ali<sup>2,3</sup>, M. Kusý<sup>1</sup>, S. Scudino<sup>2</sup>, R. Čička<sup>1</sup>, M. Drienovský<sup>1</sup>, P. Priputen<sup>1</sup>, J. Janovec<sup>1</sup>

<sup>1</sup>Slovak University of Technology, Faculty of Materials Science and Technology, Institute of Materials Science, J. Bottu 25, 917 24 Trnava, Slovak Republic

<sup>2</sup>IFW Dresden, Institut für Komplexe Materialien, Postfach 27 01 16, D-01171 Dresden, Germany

<sup>3</sup>Pakistan Institute of Engineering and Applied Sciences, P.O. Nilore, Islamabad, Pakistan

Received 28 November 2011, received in revised form 9 March 2012, accepted 4 May 2012

## Abstract

The CMA-powder and the Al-CMA composite (CMA = Al<sub>73</sub>Mn<sub>21</sub>Fe<sub>6</sub>) have been studied with the intention to characterize the influence of selected technological procedures (milling for 80 h, extrusion at 400 °C under 500 MPa, compaction at 550 °C for 0.5 h, and annealing at 550 °C for respective 0.25 and 0.5 h) on the phase evolution inside CMA-areas and at Al/CMA interfaces. In the investigation X-ray diffraction and scanning electron microscopy including energy dispersive X-ray spectroscopy were used. It was shown that CMA-powder consisting of T(HT) +  $\gamma_2$  became totally amorphous after 80 h of milling. During extrusion, compaction, and annealing of the Al-CMA composite, the originally amorphous CMA particles were found to transform into crystalline phases at the assistance of aluminium diffusion towards the CMA-area. At the Al/CMA interfaces on the CMA side, IMC-areas (IMC = intermetallic compound) were formed consisting of Al<sub>6</sub>(Mn, Fe). T(LT) + Al<sub>4</sub>(Mn, Fe) + Al<sub>6</sub>(Mn, Fe) phases were identified in the CMA-areas after the annealing of the Al-CMA composite for 0.5 h at 550 °C.

**Key words:** metal-matrix composites, interfaces, scanning electron microscopy, energy dispersive X-ray spectroscopy, extrusion, annealing

## 1. Introduction

Metal-matrix composites belong to advanced structural materials of the 21<sup>st</sup> century, because of their improved mechanical and technological properties resulting from the interaction between metallic matrix and reinforcing dispersive particles [1, 2]. It was shown the reinforcing particles contribute to higher hardness, wear resistance, tensile strength, creep behaviour of the matrix alloy [3–6]. There are many literature data available for composites consisting of the light metal matrix (e.g. Al, Mg, Ti) and ceramic reinforcing particles (e.g. SiC, Al<sub>2</sub>O<sub>3</sub>) [7–13]. However, a few literature resources are available on the light metal – complex metallic alloy (CMA) composites till now [14–18]. For instance, Qi et al. [14] investigated intermetallic phases in the hot-pressed Al-Al<sub>65</sub>Cu<sub>20</sub>Cr<sub>15</sub> compos-

ites and identified three types of quasicrystals. Tribological properties of sintered Al-CMA composites containing various volume fractions of AlCuFeB and AlCuFeCr particles were studied by Lu et al. [15]. The CMA-particles were found to improve the dry sliding wear resistance of the aluminium matrix. A positive effect of the  $\beta$ -Al<sub>3</sub>Mg<sub>2</sub> (complex metallic phase) on reinforcing the Al-based metal-matrix composites was also confirmed by Scudino et al. [18].

CMAs are characterized by high structural complexity resulting from the large number of atoms (mostly hundred to several thousand) in the unit cell [19, 20]. They exhibit, for instance, interesting electrical properties, good thermal stability, excellent chemical resistance, absorption of solar energy, and storage of hydrogen [19–22]. Even if CMAs show a high brittleness at ambient temperature, their use as

\*Corresponding author: [ivona.cernickova@stuba.sk](mailto:ivona.cernickova@stuba.sk)

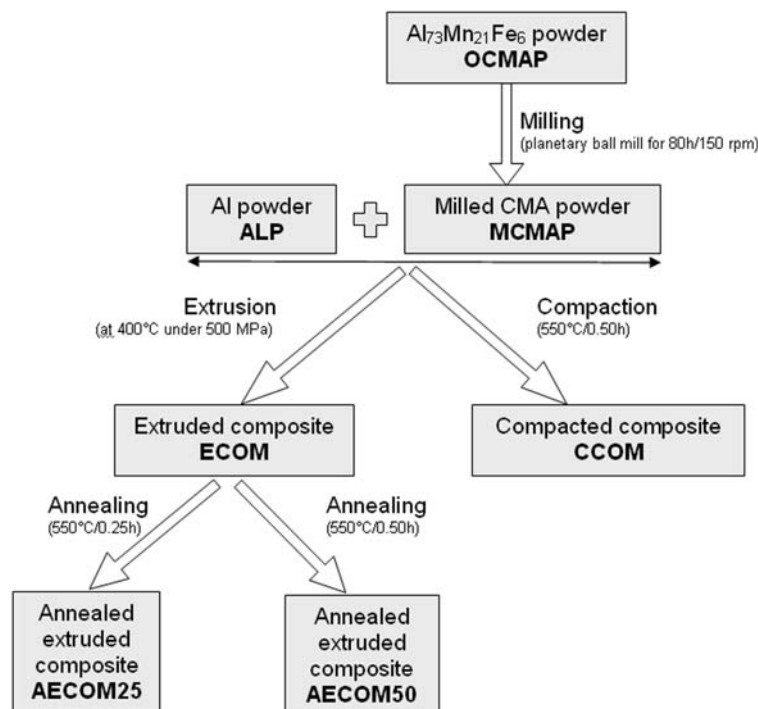


Fig. 1. Scheme showing sequence of technological operations used. Denotations of particular conditions are also given.

reinforcing particles can lead to the formation of novel composites preserving the unique properties of CMAs. Moreover, the intermetallic compounds (IMC) formed due to the deformation and thermal effects at the metal matrix – CMA interfaces can contribute to the enhanced cohesion at internal surfaces and to influence positively final properties of composites [23–29].

In this work, the CMA-powder and the Al-CMA composite (CMA =  $\text{Al}_{73}\text{Mn}_{21}\text{Fe}_6$ ) have been studied with the intention to characterize the influence of selected technological procedures (milling, extrusion, compaction, and annealing) on the phase evolution inside the CMA-areas and at the Al/CMA interfaces.

## 2. Experimental procedure

The investigated powder with the nominal composition  $\text{Al}_{73}\text{Mn}_{21}\text{Fe}_6$  (denoted also OCMAP in this work, Fig. 1) was produced by mechanical alloying of elemental powder mixtures (purity > 99.9 wt.%) using a Retsch PM400 planetary ball mill as well as hardened steel balls and vials. The powder was milled for the maximum 80 h with a ball-to-powder mass ratio (BPR) of 13 : 1 and a milling intensity of 150 rpm. To avoid or minimize a possible atmosphere contamination during milling, vial charging and a subsequent sample handling were carried out in a glove box under purified argon atmosphere (less than 1 ppm  $\text{O}_2$  and  $\text{H}_2\text{O}$ ). The elemental Al-powder of granulometric fraction below 40  $\mu\text{m}$  (ALP, Fig. 1) and the milled

$\text{Al}_{73}\text{Mn}_{21}\text{Fe}_6$  powder of granulometric fraction below 150  $\mu\text{m}$  (MCMAP, Fig. 1) were mixed and synthesized subsequently using powder metallurgy methods. The blending ratio was 3 : 2. The consolidation was done by hot extrusion under argon atmosphere at 400 °C and 500 MPa. The extrusion ratio was 6 : 1. The extruded Al- $\text{Al}_{73}\text{Mn}_{21}\text{Fe}_6$  composite (ECOM, Fig. 1) was annealed at 550 °C for 0.25 h (AECOM25, Fig. 1) and 0.5 h (AECOM50, Fig. 1) in nitrogen atmosphere using Perking Elmer Diamond differential scanning calorimeter. The compacted composite (CCOM) consisting of elemental Al powder (60 vol.%) blended with milled  $\text{Al}_{73}\text{Mn}_{21}\text{Fe}_6$  powder (40 vol.%) was prepared using uniaxial hot pressing at 550 °C for 0.5 h.

The  $\text{Al}_{73}\text{Mn}_{21}\text{Fe}_6$  powder milled for 0 h, 0.5 h, 10 h, 20 h, 30 h, 40 h, 60 h, and 80 h as well as the ECOM, CCOM, AECOM25, and AECOM50 composites were investigated using both the X-ray diffraction (XRD) and the scanning electron microscopy (SEM) including energy dispersive X-ray spectroscopy (EDX). The XRD measurements were carried out by a Philips PW 1830 diffractometer with Bragg-Brentano geometry using iron filtered  $\text{CoK}\alpha_1$  radiation at following conditions: scattering angle  $2\theta$  from 5 to 70°, step size 0.02°, and exposure time 10 s per step. For SEM/EDX studies a JEOL JSM-7600F scanning electron microscope was used operating at the acceleration voltage 20 kV in SEI (secondary electron) and BEI (back-scattered electron) regimes. The microscope is equipped with the X-max spectrometer for EDX analysis using INCA Energy software from Ox-

Table 1. Metal compositions of CMA-areas (central part) and IMC-areas (if plausible). The values for OCMAP and MCMAP are given in the same row, because of negligible differences between them

Condition	Metal composition of CMA particle – central part (at.%)			Metal composition of IMC (at.%)		
	Al	Mn	Fe	Al	Mn	Fe
OCMAP (MCMAP)	72.81 ± 1.29	20.91 ± 1.36	6.28 ± 0.57	–	–	–
ECOM	73.54 ± 1.04	20.25 ± 0.78	6.21 ± 0.42	–	–	–
CCOM	76.97 ± 1.13	18.21 ± 0.96	4.82 ± 0.28	84.96 ± 2.24	11.62 ± 1.85	3.42 ± 0.61
AECOM25	73.18 ± 0.21	20.56 ± 0.28	6.26 ± 0.23	84.55 ± 2.16	11.93 ± 1.42	3.52 ± 0.51
AECOM50	77.40 ± 1.46	17.64 ± 1.08	4.96 ± 0.32	84.98 ± 2.72	11.69 ± 2.14	3.33 ± 0.61

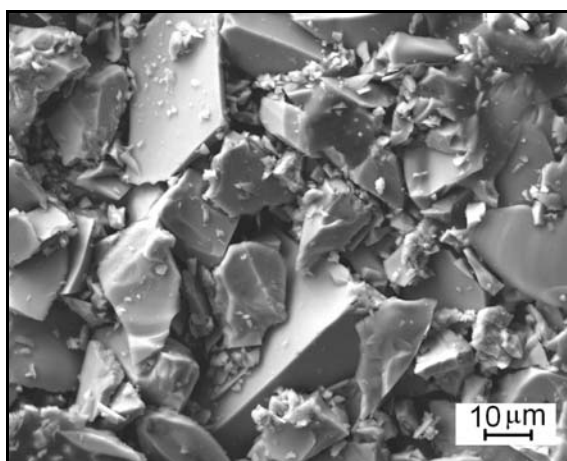


Fig. 2. SEM/BEI micrographs of  $\text{Al}_{73}\text{Mn}_{21}\text{Fe}_6$  powder (OCMAP).

ford Instruments. At least 10 measurements per microstructure constituent were carried out to calculate average values of the metal composition. Volume fractions were calculated by means of an ImageJ software designed for the precise image analysis.

### 3. Results

The SEM/BEI micrograph of OCMAP is shown in Fig. 2. The powder metal composition is given in Table 1. Powder X-ray diffraction patterns of the  $\text{Al}_{73}\text{Mn}_{21}\text{Fe}_6$  powder after milling for various times are documented in Fig. 3. Both high-temperature Taylor phase,  $T(\text{HT})$ , and smaller amount of  $\gamma_2$ -phase were identified in OCMAP (Fig. 3 and Tables 2 and 3). On milling, the amount of the amorphous phase was found to increase with increasing time. After milling for 40 h and longer, the powder became totally amorphous. The ECOM microstructure is illustrated in Fig. 4a. Besides the matrix forming 55.2 % of the total volume and CMA particles (39.6 %), also pores (5.2 %) were observed in the microstructure (Table 4).

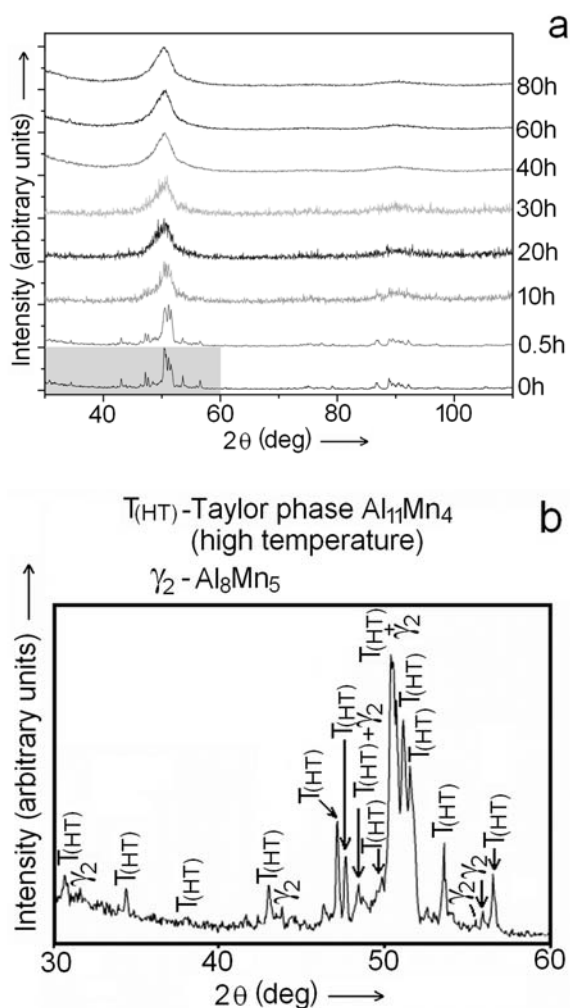


Fig. 3. Set of powder X-ray diffraction patterns corresponding to the  $\text{Al}_{73}\text{Mn}_{21}\text{Fe}_6$  powder milled for various times (a), a detail view on the grey highlighted area (b).

The same volume fractions of the aluminium matrix (around 55 %) and pores (5.2 %) as documented for the ECOM, were also found in other three compacted conditions – CCOM (Fig. 4b), AECOM25 (Fig. 4c), and AECOM50 (Fig. 4d), Table 4. In ECOM, alu-

Table 2. Structural parameters of phases identified experimentally [30, 31, 34–36]

Phase	Denotation (modification)	Pearson symbol	Al content (at.%)	Space group
Al, (Al)	–	cF4	99.48–100	Fm $\bar{3}$ m
Al <sub>11</sub> Mn <sub>4</sub> (Taylor phase)	T(HT) T(LT)	oP160 aP30	71.3–75 73	Pnma P $\bar{1}$
Al <sub>8</sub> Mn <sub>5</sub>	$\gamma_2$	hR26	50–68.6	R $\bar{3}$ m
Al <sub>4</sub> Mn (icosahedral phase)	$\mu$ $\lambda$	– –	79.2–81 81–83.2	– –
Al <sub>6</sub> Mn	Al <sub>6</sub> Mn	oC28	85.7	Cmcm

Table 3. Phases identified in particular microstructure constituents of investigated conditions

Condition	Phases identified		
	Matrix	IMC	CMA
OCMAP	–	–	T(HT), $\gamma_2$
MCMAP	–	–	amorphous
ECOM	Al	–	T(LT), amorphous
CCOM	Al, (Al)	Al <sub>6</sub> (Mn, Fe)	T(LT), Al <sub>4</sub> (Mn, Fe)
AECOM25	Al, (Al)	Al <sub>6</sub> (Mn, Fe)	T(LT), Al <sub>4</sub> (Mn, Fe)
AECOM50	Al, (Al)	Al <sub>6</sub> (Mn, Fe)	T(LT), Al <sub>4</sub> (Mn, Fe)

Table 4. Volume fractions of microstructure constituents for particular conditions

Condition	Volume fraction (%)			
	CMA	IMC layer	Al matrix	Pore
OCMAP (MCMAP)	100	–	–	–
ECOM	39.6	–	55.2	5.2
CCOM	8.7	30.8	55.3	5.2
AECOM25	15.4	24.3	55.1	5.2
AECOM50	8.1	31.2	55.5	5.2

minium, T(LT) and amorphous phases were identified (Fig. 5a, Tables 2 and 3). Some of the peaks expected for T(LT) were not observed in the diffraction pattern in Fig. 5a, the dashed line corresponds to the peak of the amorphous phase. The average metal compositions of CMA-particles for various conditions are given in Table 1.

The microstructure of CCOM (Fig. 4b) consists of three constituents corresponding to the aluminium matrix (dark grey) and the CMA-area (bright grey and white). The white constituent corresponds to the modified CMA formed with T(LT) and icosahedral Al<sub>4</sub>(Mn, Fe) (Fig. 5b, Tables 2 and 3). The bright grey constituent was identified as a newly formed IMC of the Al<sub>6</sub>(Mn, Fe) structure (Fig. 5b, Tables

2 and 3). The volume fraction of IMC was found to be around 3.5 times higher than that of the modified CMA (Table 4). The modified CMA was found to contain more Al and less Mn and Fe than the original CMA in OCMAP and ECOM conditions (Table 1). In the annealed conditions (AECOM25, AECOM50), the same microstructure constituents (compare Figs. 4b–d) and phases (Table 2) were found as documented for CCOM. The volume fractions and metal compositions of particular microstructure constituents corresponding to CCOM and AECOM50 are comparable, contrary to the AECOM25 condition. The metal composition of the modified CMA in the latter condition is similar to those of the original CMA in OCMAP and ECOM.

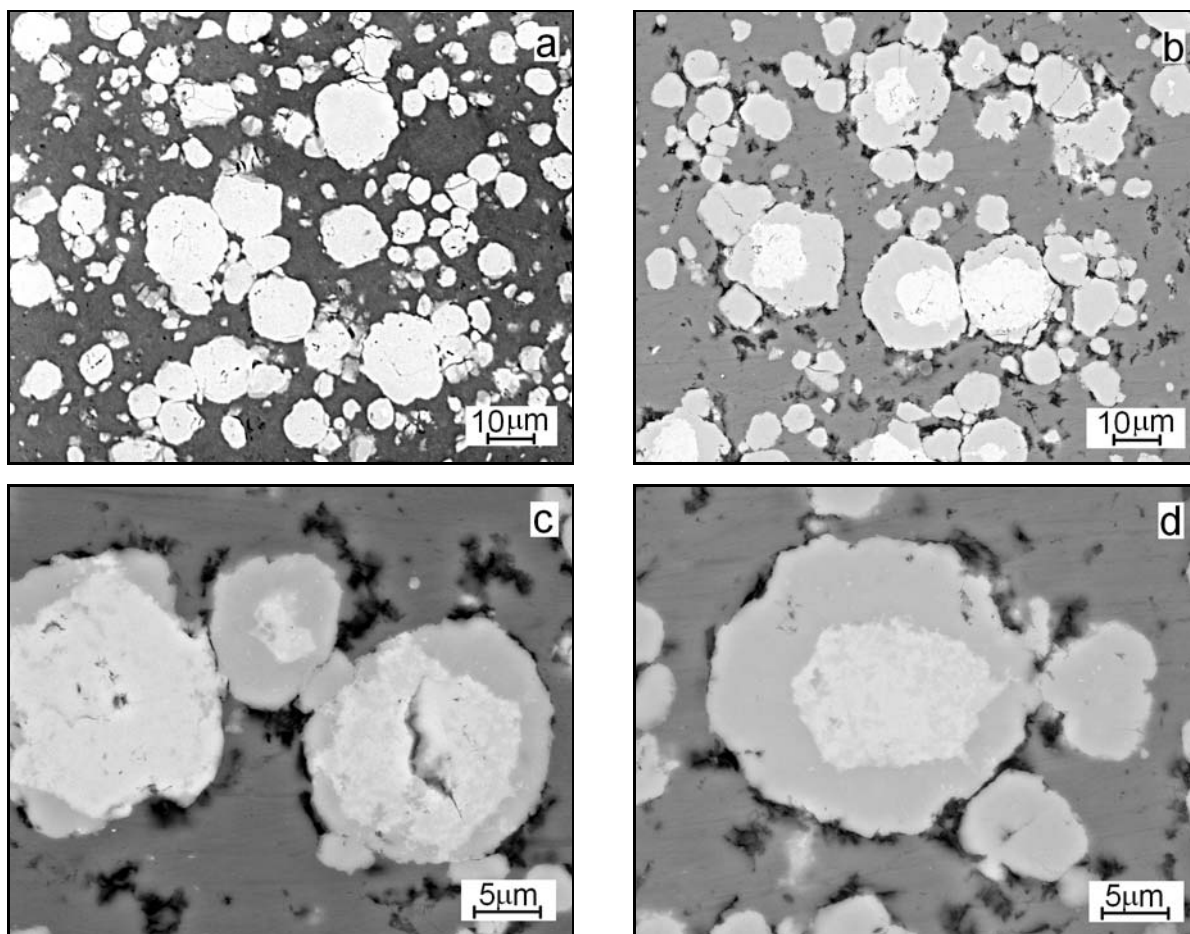


Fig. 4. SEM/BEI micrographs showing distribution of particular microstructure constituents in ECOM (a), CCOM (b), AECOM25 (c), and AECOM50 (d) conditions.

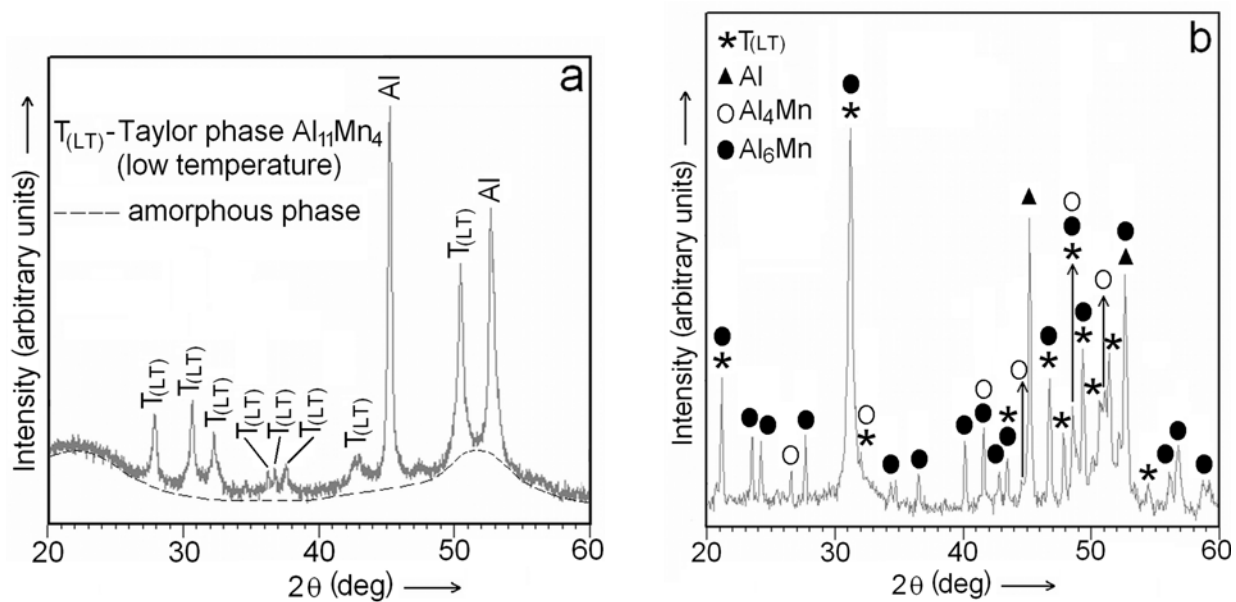


Fig. 5. Powder X-ray diffraction patterns corresponding to ECOM (a) and CCOM (b). In diffraction patterns, simple notations  $\text{Al}_4\text{Mn}$  and  $\text{Al}_6\text{Mn}$  are used for the  $\text{Al}_4(\text{Mn, Fe})$  and  $\text{Al}_6(\text{Mn, Fe})$  phases, respectively. Similarly,  $\text{Al}_{11}\text{Mn}_4$  stands for  $\text{Al}_{11}(\text{Mn, Fe})_4$ .

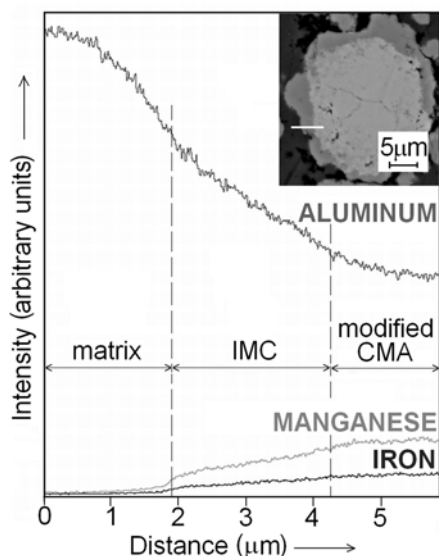


Fig. 6. Compositional changes along the solid line marked in small window in upper right corner of the basic diagram; documented for AECOM25.

#### 4. Discussion

Altogether seven phases were identified in the conditions investigated. Four of them, T(HT),  $\gamma_2$ , T(LT), and amorphous, are related directly to the transformations taking place in the original CMA-particles (Fig. 2). Other two phases,  $\text{Al}_4(\text{Mn, Fe})$  and  $\text{Al}_6(\text{Mn, Fe})$ , were also found in the CMA-area, but their formation was conditioned by a diffusion of aluminium from the matrix towards this area. This suggestion is in agreement with the data available in concerned phase diagrams [30, 31]. The last identified phase, Al or (Al), represents the matrix in the composite. An indirect evidence about the aluminium diffusion towards the CMA-area resides in higher aluminium contents in the newly formed  $\text{Al}_4(\text{Mn, Fe})$  and  $\text{Al}_6(\text{Mn, Fe})$  compounds compared to the  $\text{Al}_{73}\text{Mn}_{21}\text{Fe}_6$  alloy [26, 29]. On the other hand, there was not observed any step change in Mn and Fe concentrations near the IMC/matrix interface (Fig. 6). Thus, traces of Mn and Fe could occur on the matrix side of this interface. In spite of the limited solubility and diffusivity of Mn and Fe in aluminium at 550 °C ( $D_{\text{Mn}/\text{Al}(550^\circ\text{C})} = 3.1823 \times 10^{-16} \text{ m}^2 \text{ s}^{-1}$  and  $D_{\text{Fe}/\text{Al}(550^\circ\text{C})} = 1.2144 \times 10^{-14} \text{ m}^2 \text{ s}^{-1}$ ) [30–34], a narrow layer of the dilute Al(Mn, Fe) solid solution (hardly identifiable by experiment) is expected to be formed on the matrix side.

Original CMA-particles (Fig. 1) overcame the strongest structural changes during milling. As it is summarized in Table 2, their microstructure consisting of T(HT) and  $\gamma_2$  before milling was transformed in totally amorphous microstructure after 80 h

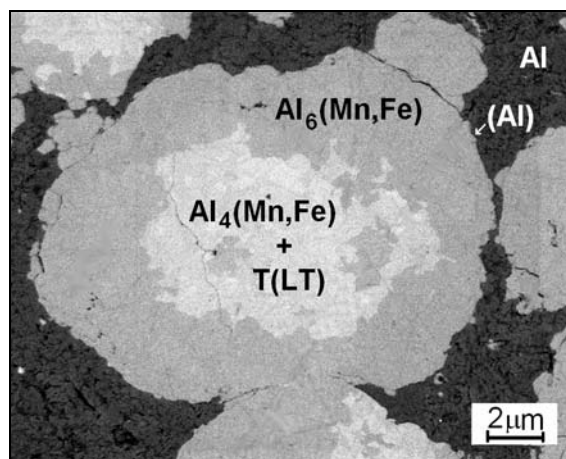


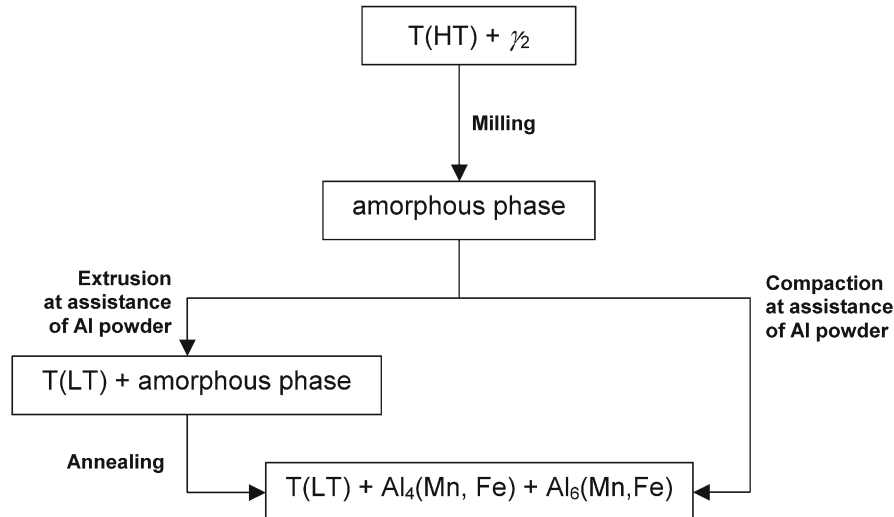
Fig. 7. SEM/BEI micrograph showing detail view on microstructure constituents in CCOM. Phases identified in particular constituents are also given.

of milling (Fig. 3). On extrusion at 400 °C, the amorphous phase as a part of Al-CMA composite transformed into T(LT) partially. The matrix aluminium was not observed to participate in this transformation, because of identical metal compositions of CMA-areas in OCMAP and ECOM conditions (Table 1). On the other hand, the compaction of the ALP + MCMAP sample at 550 °C for 0.5 h led to the interaction between the matrix aluminium and the amorphous CMA phase. As a result, the amorphous phase disappeared. The central part of the original CMA was modified into T(LT) +  $\text{Al}_4(\text{Mn, Fe})$ , and the outer part transformed into the single-phase IMC-area consisting of  $\text{Al}_6(\text{Mn, Fe})$ , Fig. 7. The annealing of the extruded condition (ECOM) at 550 °C for 0.5 h (AECOM50) led to the formation of the same phases showing the same volume fractions and metal compositions as it was reported for the annealed CCOM condition (Tables 1, 2, 4). The annealed AECOM25 and AECO50 conditions showed differences in both volume fractions and metal compositions (Tables 1 and 4) that confirm the significance of annealing time for the microstructure formation.

The IMC-areas exhibited gradients in Al, Mn, and Fe concentrations. The highest contents of Mn and Fe were found at the IMC/CMA interface, the lowest contents at the IMC/matrix interface (Fig. 6). Similar findings were also published by Arsenault [27] for the metal-matrix Al-SiC composite. The mentioned gradients did not cause any significant heterogeneity in the average metal compositions of the concerned elements. A growth in the volume fraction of IMC at the expense of the modified CMA with increasing annealing time (compare AECOM25 and AECOM50 conditions, Figs. 4c,d) have shown that the single-phase  $\text{Al}_6(\text{Mn, Fe})$  microstructure seems to be more stable than the T(LT) +  $\text{Al}_4(\text{Mn, Fe})$  microstructure at 550 °C. It can

be explained with the aluminium diffusion towards the CMA-area and the subsequent shift of the equilibrium to the Al-rich corner in concerned binary and ternary phase diagrams [30, 34–36]. Thus, the CMA-area can be formed with  $\text{Al}_6(\text{Mn, Fe})$  only if the annealing is prolonged over 0.5 h.

The above findings make possible to propose the sequence of phase transformations taking place in the CMA-area during technological procedures considered:



## 5. Conclusions

The results concerning the evolution of phases in both the CMA-powder on milling for maximum 80 h as well as the Al-CMA composite ( $\text{CMA} = \text{Al}_{73}\text{Mn}_{21}\text{Fe}_6$ ) after extruding (400 °C, 500 MPa), compacting (550 °C, 0.5 h), and/or annealing of extruded samples (550 °C, 0.25 and 0.5 h) can be summarized as follows:

1. The double-phase microstructure of original CMA-particles consisting of  $\text{T(HT)} + \gamma_2$  was found to transform into totally amorphous microstructure after 80 h of milling.

2. The amorphous CMA-areas in the Al-CMA composite overcame structural changes during extrusion, compaction, and annealing at the assistance of aluminium diffusion towards the CMA-area.

3. On extrusion, a partial transformation of amorphous CMA into  $\text{T(LT)}$  was observed. Both the annealing of the extruded sample at 550 °C for 0.5 h and the compaction of the powder sample at the same time-temperature parameters led to the formation of the  $\text{T(LT)} + \text{Al}_4(\text{Mn, Fe}) + \text{Al}_6(\text{Mn, Fe})$  microstructure within the CMA-area.

4. The single-phase IMC-area consisting of  $\text{Al}_6(\text{Mn, Fe})$  was formed at the CMA/matrix interface on the CMA side. The growth in volume fraction of IMC at the expense of  $\text{T(LT)} + \text{Al}_4(\text{Mn, Fe})$  was observed at 550 °C with increasing the annealing time.

## Acknowledgements

The research done in this work was financed by the European Regional Development Fund (ERDF) under the project No. ITMS:26220120014 “Centre for development and application of advanced diagnostic methods in processing of metallic and non-metallic materials” of the Research & Development Operational Programme, and by the Grant Agency of the Ministry of Education of the Slovak Republic and the Slovak Academy of Sciences (VEGA) under the contracts No. 1/0011/10. The authors would like to thank Prof. Dr. Jürgen Eckert of the Leibniz Institute for Solid State and Materials Research in Dresden for giving valuable advices on completing the manuscript.

## References

- [1] Scudino, S., Liu, G., Prashanth, K. G., Bartusch, B., Surreddi, K. B., Murty, B. S., Eckert, J.: *Acta Materialia*, 57, 2009, p. 2029.
- [2] Miracle, D. B.: *Composites Science and Technology*, 65, 2005, p. 2526.  
[doi:10.1016/j.compscitech.2005.05.027](https://doi.org/10.1016/j.compscitech.2005.05.027)
- [3] Dinaharan, I., Murugan, N., Parameswaran, S.: *Materials Science and Engineering, A* 528, 2011, p. 5733.
- [4] Douin, J., Donnadieu, P., Finel, A., Dirras, G. F., Silvain, J. F.: *Composites, A* 33, 2002, p. 1397.
- [5] Doel, T. J. A., Loretto, M. H., Bowen, P.: *Composites*, 24, 1993, p. 270. [doi:10.1016/0010-4361\(93\)90174-7](https://doi.org/10.1016/0010-4361(93)90174-7)
- [6] Li, Y., Langdon, T. G.: *Acta Materialia*, 45/11, 1997, p. 4797.
- [7] Rodríguez, J., Poza, P., Garrido, M. A., Rico, A.: *Wear*, 262, 2007, p. 292.  
[doi:10.1016/j.wear.2006.05.006](https://doi.org/10.1016/j.wear.2006.05.006)

- [8] Deuis, R. L., Subramanian, C., Yellup, J. M.: Composites Science and Technology, *57*, 1997, p. 415. [doi:10.1016/S0266-3538\(96\)00167-4](https://doi.org/10.1016/S0266-3538(96)00167-4)
- [9] Prasad, B. K.: Wear, *262*, 2007, p. 262. [doi:10.1016/j.wear.2006.05.004](https://doi.org/10.1016/j.wear.2006.05.004)
- [10] Tabandeh Khorshid, M., Jenabali Jahromi, S. A., Moshksar, M. M.: Materials and Design, *31*, 2010, p. 3880. [doi:10.1016/j.matdes.2010.02.047](https://doi.org/10.1016/j.matdes.2010.02.047)
- [11] Inouea, M., Nagaob, U. H., Suganumaa, K., Niiharaa, K.: Materials Science and Engineering, *A258*, 1998, p. 298. [doi:10.1016/S0921-5093\(98\)00948-4](https://doi.org/10.1016/S0921-5093(98)00948-4)
- [12] Davidson, A. M., Regener, D.: Composites Science and Technology, *60*, 2000, p. 865. [doi:10.1016/S0266-3538\(99\)00151-7](https://doi.org/10.1016/S0266-3538(99)00151-7)
- [13] Poddar, P., Srivastava, V. C., De, P. K., Sahoo, K. L.: Materials Science and Engineering, *A 460–461*, 2007, p. 357. [doi:10.1016/j.msea.2007.01.052](https://doi.org/10.1016/j.msea.2007.01.052)
- [14] Qi, Y. H., Zhang, Z. P., Hei, Z. K., Dong, C.: Journal of Alloys and Compounds, *285*, 1999, p. 221. [doi:10.1016/S0925-8388\(98\)01041-X](https://doi.org/10.1016/S0925-8388(98)01041-X)
- [15] Lu, D., Celis, J. P., Kenzari, S., Fournée, V., Zhou, D. B.: Wear, *270*, 2011, p. 528. [doi:10.1016/j.wear.2011.01.007](https://doi.org/10.1016/j.wear.2011.01.007)
- [16] CHENG, S., YANG, G., ZHU, M., WANG, J., ZHOU, Y.: Transactions of Nonferrous Metals, Society of China, *20*, 2010, p. 572.
- [17] Lee, S. M., Jung, J. H., Fleury, E., Kim, W. T., Kim, D. H.: Materials Science and Engineering, *294*, 2000, p. 99. [doi:10.1016/S0921-5093\(00\)01223-5](https://doi.org/10.1016/S0921-5093(00)01223-5)
- [18] Scudino, S., Liu, G., Sakaliyska, M., Surreddi, K. B., Eckert, J.: Acta Materialia, *57*, 2009, p. 4529. [doi:10.1016/j.actamat.2009.06.017](https://doi.org/10.1016/j.actamat.2009.06.017)
- [19] Urban, K., Feuerbacher, M.: Journal of Non-Crystalline Solids, *334&335*, 2004, p. 143.
- [20] Dubois, J. M.: Journal of Physics: Condensed Matter, *13*, 2001, p. 7753. [doi:10.1088/0953-8984/13/34/318](https://doi.org/10.1088/0953-8984/13/34/318)
- [21] Urban, K., Feuerbacher, M.: Journal of Non-Crystalline Solids, *334&335*, 2004, p. 143.
- [22] Dubois, J. M.: Nat. Mater., *9*, 2010, p. 287. PMID:20332784. [doi:10.1038/nmat2737](https://doi.org/10.1038/nmat2737)
- [23] Tham, L. M., Gupta, M., Cheng, L.: Journal of Materials Processing Technology, *89–90*, 1999, p. 128. [doi:10.1016/S0924-0136\(99\)00002-3](https://doi.org/10.1016/S0924-0136(99)00002-3)
- [24] Kang, C. G., Seo, Y. H.: Journal of Materials Processing Technology, *61*, 1996, p. 241. [doi:10.1016/0924-0136\(95\)02180-9](https://doi.org/10.1016/0924-0136(95)02180-9)
- [25] Barmouza, M., Kazem, M., Givvia, B., Seyfi, J.: Materials Characterization, *62*, 2011, p. 108. [doi:10.1016/j.matchar.2010.11.005](https://doi.org/10.1016/j.matchar.2010.11.005)
- [26] Ilo, S., Just, Ch., Badisch, E., Wosik, J., Danninger, H.: Materials Science and Engineering, *A 527*, 2010, p. 6378. [doi:10.1016/j.msea.2010.06.060](https://doi.org/10.1016/j.msea.2010.06.060)
- [27] Arsenault, R. J.: Composites, *25*, 1994, p. 540. [doi:10.1016/0010-4361\(94\)90182-1](https://doi.org/10.1016/0010-4361(94)90182-1)
- [28] Cao, G. H., Liu, Z. G., Liu, J. M., Shen, G. J., Wu, S. Q.: Composite Science and Technology, *61*, 2001, p. 545.
- [29] Zhu, H. X., Abbaschian, R.: Materials Science and Engineering, *A282*, 2000, p. 1. [doi:10.1016/S0921-5093\(99\)00788-1](https://doi.org/10.1016/S0921-5093(99)00788-1)
- [30] Raghavan, V.: Journal of Phase Equilibria and Diffusion, *28*, 2007, p. 410. [doi:10.1007/s11669-007-9121-y](https://doi.org/10.1007/s11669-007-9121-y)
- [31] Liu, X. J., Ohnuma, I., Kainuma, R., Ishida, K.: Journal of Phase Equilibria, *20*, 1999, p. 45. [doi:10.1361/105497199770335938](https://doi.org/10.1361/105497199770335938)
- [32] Du, Y., Chang, Y. A., Huang, B., Gong, W., Jin, Z., Xu, H., Yuan, Z., Liu, Y., He, Y., Xie, F.-Y.: Materials Science and Engineering, *A363*, 2003, p. 140.
- [33] Neumann, G., Tuijn, C.: Self-diffusion and Impurity Diffusion in Pure Metals. Handbook of Experimental Data. Amsterdam, Elsevier 2008.
- [34] Okamoto, H.: Journal of Phase Equilibria, *18*, 1997, p. 399.
- [35] Pavlyuchkov, D., Balanetsky, S., Kowalski, W., Surowiec, M., Grushko, B.: Journal of Alloys and Compounds, *477*, 2009, p. L41. [doi:10.1016/j.jallcom.2008.11.005](https://doi.org/10.1016/j.jallcom.2008.11.005)
- [36] Kreiner, G., Franzen, H. F.: Journal of Alloys and Compounds, *261*, 1997, p. 83. [doi:10.1016/S0925-8388\(97\)00213-2](https://doi.org/10.1016/S0925-8388(97)00213-2)